

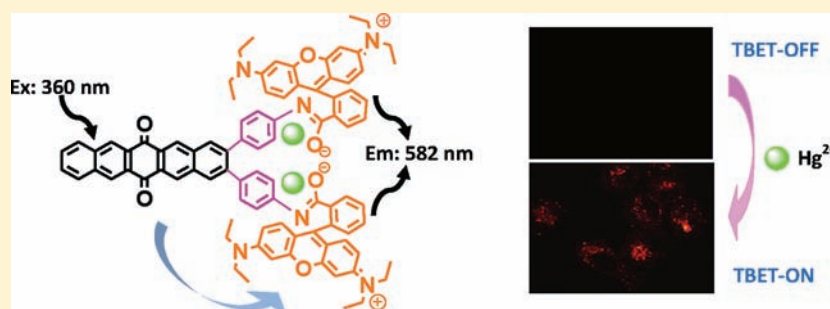
New Fluorogenic Sensors for Hg²⁺ Ions: Through-Bond Energy Transfer from Pentaquinone to Rhodamine

Vandana Bhalla,^{*,†} Roopa,[†] Manoj Kumar,^{*,†} Parduman Raj Sharma,[‡] and Tandeep Kaur[‡]

[†]Department of Chemistry, UGC Sponsored-Centre for Advanced Studies-I, Guru Nanak Dev University, Amritsar 143005, Punjab, India

[‡]Department of Cancer Pharmacology, Indian Institute of Integrative Medicine, Canal Road, Jammu 180001, India

S Supporting Information



ABSTRACT: New pentaquinone derivatives **5** and **8** having rhodamine moieties have been designed and synthesized that undergo through-bond energy transfer (TBET) in the presence of Hg²⁺ ions among the various cations (Cu²⁺, Pb²⁺, Fe²⁺, Fe³⁺, Zn²⁺, Ni²⁺, Cd²⁺, Co²⁺, Ag⁺, Ba²⁺, Mg²⁺, K⁺, Na⁺, and Li⁺) tested in mixed aqueous media.

INTRODUCTION

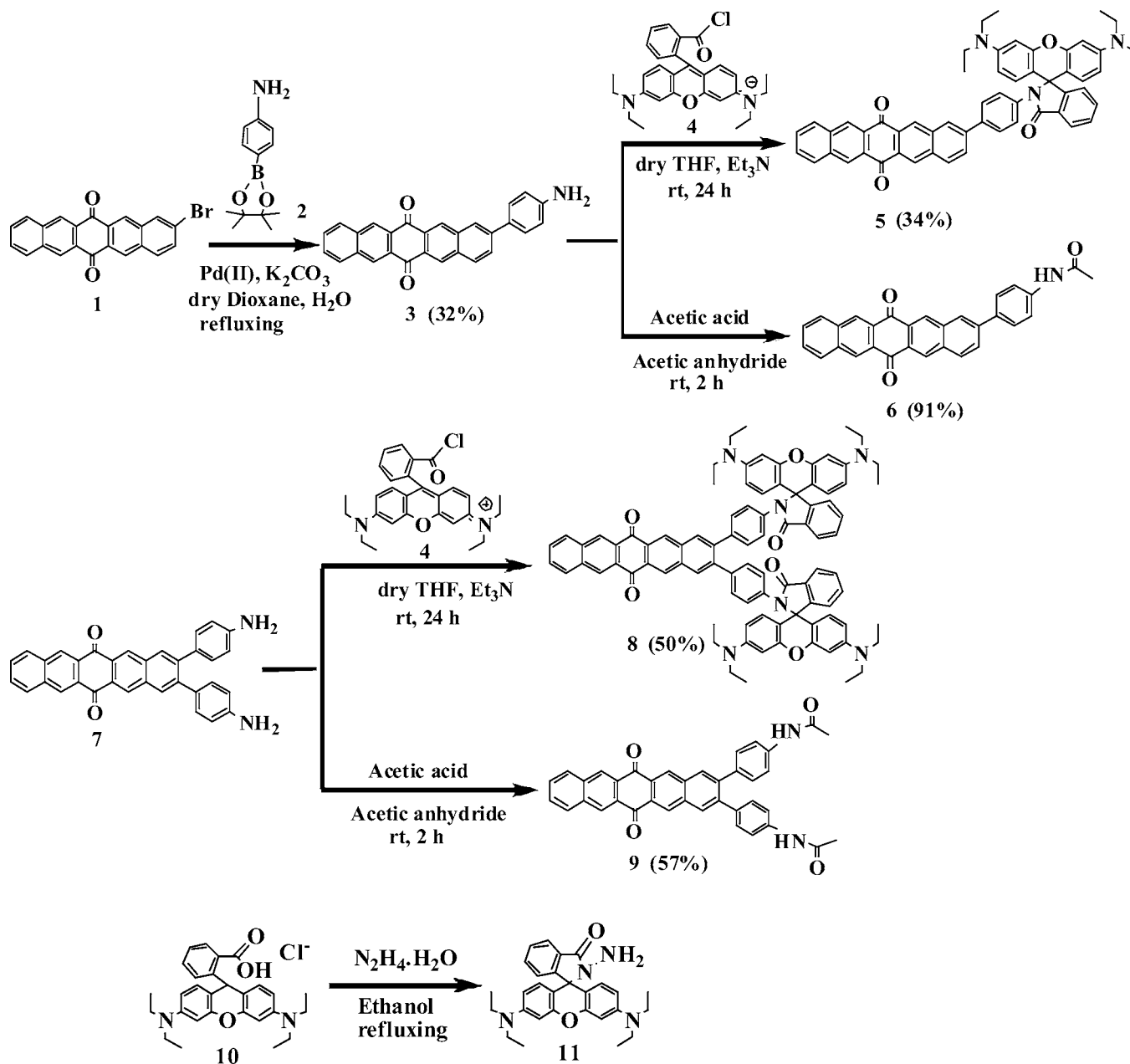
The developments of fluorogenic sensors for heavy and soft transition-metal ions, based on ion-induced changes in fluorescence, are particularly attractive because of their simplicity, high sensitivity, and instantaneous response.¹ Among soft transition-metal ions, mercury has received considerable attention because it is highly toxic. The widespread contamination of mercury is due to a variety of natural and anthropogenic sources,² including oceanic and volcanic emission,^{3,4} solid waste incineration, combustion of fossil fuels,⁵ and gold mining.⁶ The Environmental Protection Agency (EPA) standard for the maximum allowable level of inorganic mercury(II) in drinking water is 2 ppb.⁵ Thus, exposure to mercury, even at very low concentration, leads to digestive, kidney, and especially neurological diseases.⁷ Further both elemental and ionic mercury can be converted into methylmercury by bacteria in the environment that enters the food chain and accumulates in the higher organisms,⁸ which can cause serious damage to the central nervous and endocrine systems.⁹ Thus, imaging of Hg²⁺ ions in living cells is crucial. Keeping in mind the ill effects of mercury in day-to-day life, there is a need to develop an approach for simple and rapid tracking of mercury ions in biological, toxicological, and environmental monitoring. Fluorescence spectroscopy lends a helping hand for the sensing and imaging of trace amounts of mercury because of its high sensitivity and simplicity. Mercury-selective fluorescent sensors have been reported in the past where in most cases the presence of mercury causes fluorescence quenching of the fluorophores via the spin–

orbit coupling effect.¹⁰ Fluorescence quenching not only is disadvantageous for a high signal output upon recognition but also hampers temporal separation of spectrally similar complexes with time-resolved fluorometry.¹¹ On the other hand, the sensors that undergo fluorescence enhancement in the presence of metal ions are preferred because these allow a lower detection limit and high-speed spatial resolution via microscopic imaging.^{12,13} Recently, a number of sensors based on rhodamine have been reported that show a selective “turn-on” response in the presence of Hg²⁺ ions.¹⁴ However, the rhodamine-based sensors have the limitation of having a very small Stokes shift (around 25 nm), which may lead to self-quenching and fluorescence detection errors because of excitation back-scattering effects.¹⁵ Thus, it is important to have sensors with improved properties; however, it is difficult to design such types of organic dyes with desirable photophysical properties. Recently, the possibility of having organic dyes with more than one fluorophore linked through a nonconjugated linker with an energy donor–acceptor combination has been explored wherein energy from one fluorophore, called the donor, is transferred to another fluorophore, called the acceptor, without emission of a photon.¹⁶ However, fluorescence resonance energy transfer based systems require that the donor emission overlap with the acceptor absorption, which makes their utility limited. On the other hand, through-bond energy transfer (TBET) is

Received: September 10, 2011

Published: February 2, 2012

Scheme 1. Synthesis of Compounds 3, 5, 6, 8, and 9



theoretically not subjected to the requirement of spectral overlap between the donor emission and acceptor absorption and is expected to have large Stokes and emission shifts.¹⁷ These spectral benefits are very important for the use of fluorescent dyes in chemistry, biology, medicine, and materials science. In TBET systems, the donor and acceptor are joined by a conjugated spacer, which prevents them from becoming flat and conjugated. These types of systems absorb at a wavelength characteristic of the donor and then emit via a receptor. Recently, Burgess et al.^{17a,b} have developed excellent TBET systems based on rhodamine and fluorescein for use in biotechnology, but there is only one report of such systems for fluorogenic sensing of metal ions.¹⁸ Thus, there is considerable scope for the development of fluorogenic sensors for different types of analytes that involve TBET.

RESULTS AND DISCUSSION

Our research program involves the design, synthesis, and evaluation of novel artificial receptors selective for soft metal ions and anions of clinical and environmental interest.¹⁹ In a preliminary communication from our laboratory, we reported a naphthalimide–rhodamine fluorescent dyad that undergoes TBET in the presence of Hg^{2+} ions; however, the energy transfer was not 100% because of leakage of some fluorescence from the naphthalimide donor.¹⁸ Now, in a continuation of this work, we have designed and synthesized a rhodamine–pentaquinone dyad and a rhodamine–pentaquinone–rhodamine triad, both of which undergo TBET in the presence of Hg^{2+} ions with nearly 100% efficiency. In addition, one of the two sensors can be used for imaging Hg^{2+} ions in living cells. Pentaquinone derivatives have found immense utility in the design and synthesis of solution-processable functionalized pentacene derivatives.²⁰ The role of pentaquinone as a

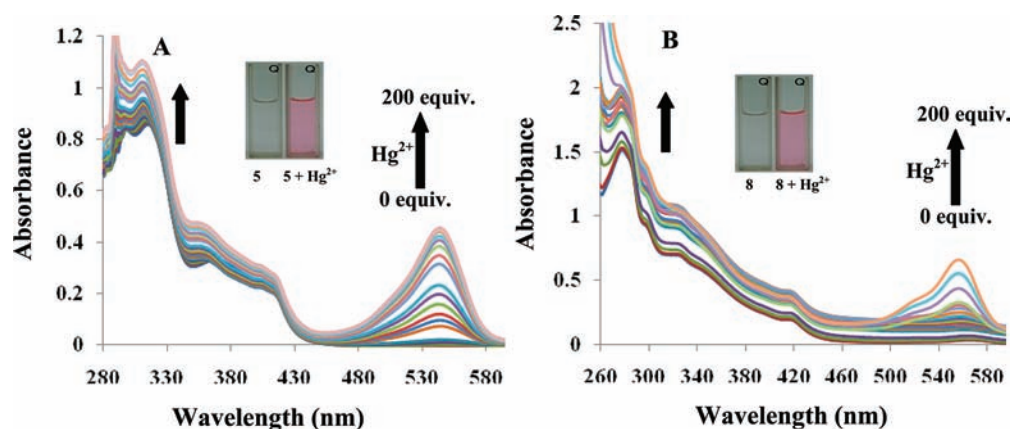


Figure 1. (A) UV-vis spectra of **5** ($10\ \mu\text{M}$) in the presence of Hg^{2+} ions (0–200 equiv) in THF/ H_2O (9.5:0.5, v/v) buffered with HEPES, pH = 7. Inset: Change in the color of the receptor before and after the addition of Hg^{2+} ions. (B) UV-vis spectra of **8** ($10\ \mu\text{M}$) in the presence of Hg^{2+} ions (0–200 equiv) in THF/ H_2O (9.5:0.5, v/v) buffered with HEPES, pH = 7. Inset: Change in the color of the receptor before and after the addition of Hg^{2+} ions.

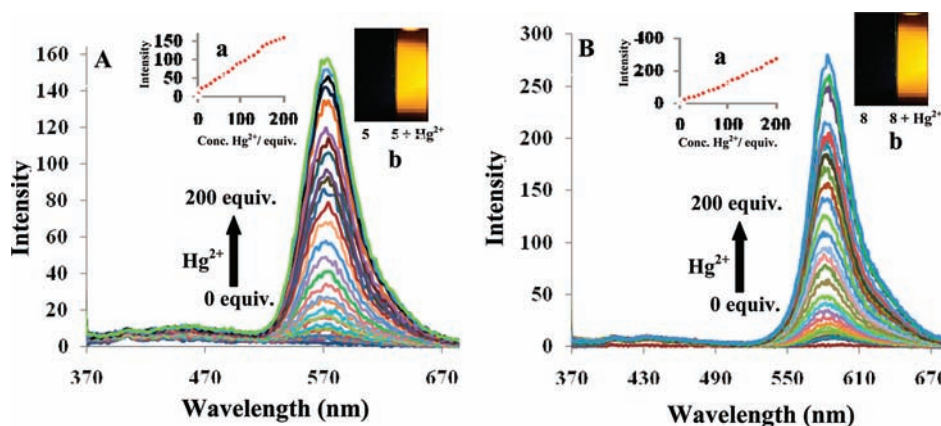


Figure 2. (A) Fluorescence response of receptor **5** ($10\ \mu\text{M}$) upon the addition of Hg^{2+} ions (0–200 equiv) in THF/ H_2O (9.5:0.5, v/v) buffered with HEPES, pH = 7; $\lambda_{\text{ex}} = 360\ \text{nm}$. Inset: (a) Change in the fluorescence intensity of receptor **5** as a function of the Hg^{2+} ion concentration. (b) Fluorescence before and after the addition of Hg^{2+} ions. (B) Fluorescence response of receptor **8** ($10\ \mu\text{M}$) upon the addition of Hg^{2+} ions (0–200 equiv) in THF/ H_2O (9.5:0.5, v/v) buffered with HEPES, pH = 7; $\lambda_{\text{ex}} = 360\ \text{nm}$. Inset: (a) Change in the fluorescence intensity of receptor **8** as a function of the Hg^{2+} ion concentration. (b) Fluorescence before and after the addition of Hg^{2+} ions.

chemosensor for different metal ions has not yet been explored, except for one report from our group.²¹ To the best of our knowledge, this is the first report where a pentaquinone scaffold has been appended with rhodamine moieties for selective sensing of Hg^{2+} ions that involve energy transfer through a conjugated spacer.

The Suzuki–Miyaura cross-coupling of boronic ester **2**²² with 2-bromo-6,13-pentacenequinone (**1**)²³ catalyzed by $\text{Pd}(\text{Cl})_2(\text{PPh}_3)_2$ furnished compound **3** in 32% yield (Scheme 1). The ^1H NMR spectrum of compound **3** showed two doublets at 6.84 and 7.94 ppm, three multiplets at 7.59–7.73, 8.12–8.16, and 8.93–8.98 ppm, one singlet at 8.24 ppm corresponding to aromatic protons, and one broad signal corresponding to amino protons at 3.89 ppm (Supporting Information, Figure S1). The mass spectrometry (MS) spectrum of compound **3** showed a parent ion peak at m/z 400.1 $[(M + 1)^+]$; Supporting Information, Figure S2]. The reaction of pentaquinone amines **3** and **7**²¹ with rhodamine acid chloride **4**²⁴ in tetrahydrofuran (THF) furnished compounds **5** and **8** in 34% and 50% yields, respectively (Scheme 1). The structures of compounds **5** and **8** were confirmed from their spectroscopic and analytical data (Supporting Information, Figures S3–S8). The ^1H NMR spectrum of compound **5/8** showed one triplet at 1.16/1.11

ppm and one quartet at 3.29–3.37/3.26–3.33 ppm corresponding to *N*-ethyl protons and three doublets at 6.69, 7.08, 7.17/6.61, 6.83, and 6.94 ppm and six multiplets at 6.28–6.36, 7.50–7.53, 7.68–7.70, 7.71–7.82, 8.02–8.16, 8.88–8.92/6.28–6.31, 7.15–7.17, 7.49–7.51, 7.68–7.71, 8.00–8.02, and 8.10–8.13 ppm corresponding to aromatic protons. In addition, compound **8** showed three singlets at 7.96, 8.86, and 8.93 ppm corresponding to aromatic protons. In the MS spectra, the parent ion peaks for compounds **5** and **8** were observed at 824.3 $[(M + 1)^+]$ and 1338.4 $[(M)^+]$ ppm, respectively. These spectroscopic data corroborate with structures **5** and **8**.

The binding behavior of compounds **5** and **8** toward different cations (Cu^{2+} , Hg^{2+} , Fe^{2+} , Fe^{3+} , Co^{2+} , Pb^{2+} , Zn^{2+} , Ni^{2+} , Cd^{2+} , Ag^+ , Ba^{2+} , Mg^{2+} , K^+ , Na^+ , and Li^+) as their perchlorate salts was investigated by UV-vis and fluorescence spectroscopy. The UV-vis spectrum of compound **5/8** exhibits absorption bands at 290/275 and 320/322 nm in THF/ H_2O (9.5:0.5, v/v) due to the pentaquinone moiety (Figure 1A/B). However, upon the addition of Hg^{2+} ions (0–200 equiv), the intensities of these absorption bands increase and a new band appears at 538/554 nm for receptor **5/8**, respectively (Figure 1A/B). These changes are accompanied by a gradual change of the color from colorless to pink, visible to the naked eye (inset,

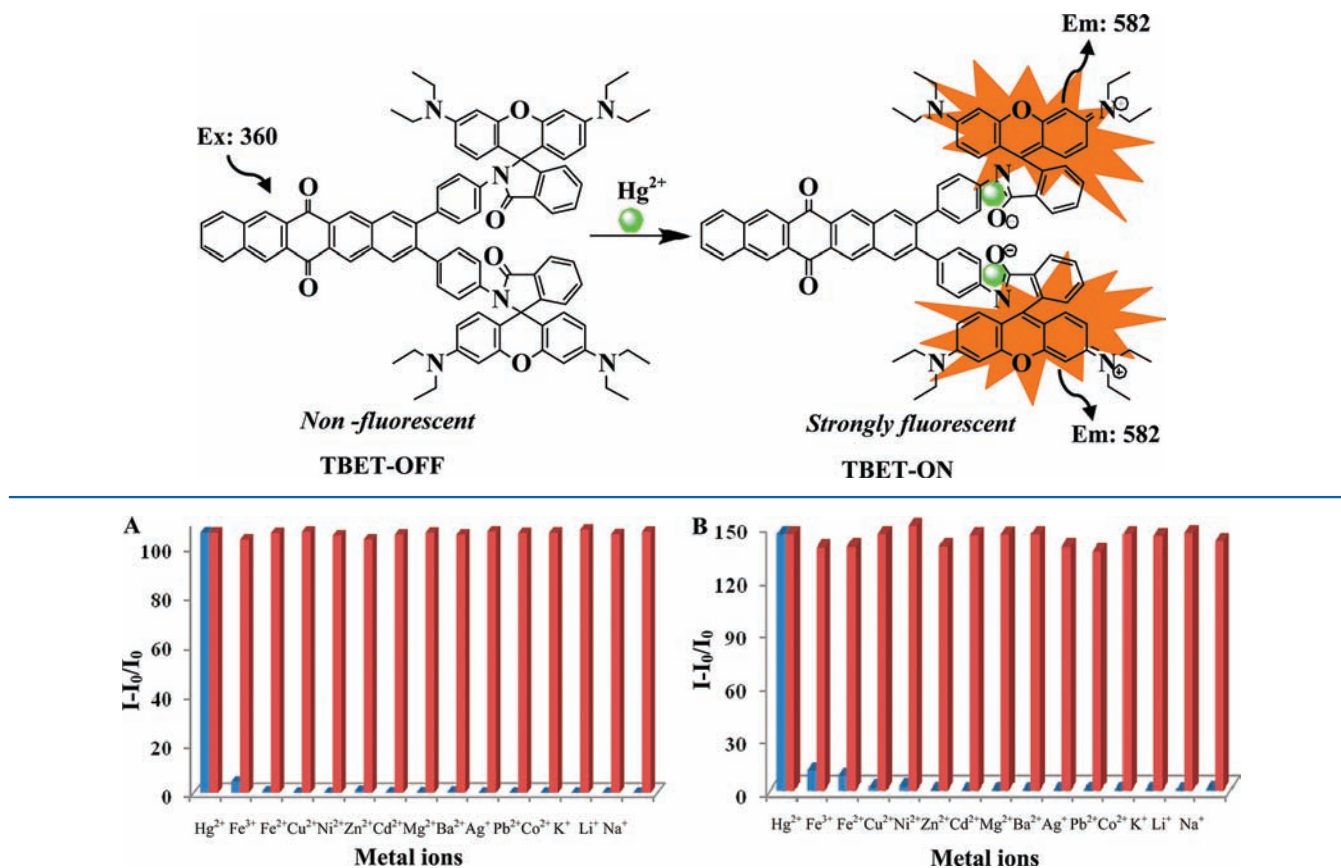
Scheme 2. Hg²⁺-Induced TBET-OFF-ON

Figure 3. (A) Fluorescence response of receptor 5 (10 μM) upon the addition of various cations (200 equiv) in THF/H₂O (9.5:0.5, v/v) buffered with HEPES, pH = 7; λ_{ex} = 360 nm. (B) Fluorescence response of receptor 8 (10 μM) upon the addition of various cations (200 equiv) in THF/H₂O (9.5:0.5, v/v) buffered with HEPES, pH = 7; λ_{ex} = 360 nm. Bars represent the emission intensity ratio ($I - I_0/I_0$). I_0 is the fluorescence intensity of each free host, and I is the fluorescence intensity after the addition of metal ions. The blue bars represent the addition of various metal ions, while the red bars represent the change in the emission that occurs upon the subsequent addition of Hg²⁺ (200 equiv) to the above solution.

Figure 1A/B). The formation of a new band at 538/554 nm is attributed to the interaction of Hg²⁺ ions with the receptor 5/8, leading to the opening of the spirolactam ring. Thus, in the presence of mercury ions, receptors 5 and 8 show the absorption characteristics of both donor and acceptor components. We also carried out UV-vis studies of model compounds 6 and 9 (pentaquinone donor) and rhodamine acceptor 11²⁵ (Supporting Information, Figures S9–S11 and S12–S16) with Hg²⁺ ions independently. These compounds exhibit similar results under experimental conditions parallel with those for receptors 5 and 8 in which two moieties are covalently linked to each other through a conjugated spacer, thus suggesting the absence of any electronic interaction between pentaquinone and rhodamine moieties in receptors 5 and 8 in the ground state in the presence of Hg²⁺ ions. In other words, receptors 5 and 8 behave like a cassette and not as a planar conjugated dye. However, no significant variation in the absorption spectra was observed in the presence of other metal ions (Cu²⁺, Fe²⁺, Fe³⁺, Co²⁺, Pb²⁺, Zn²⁺, Ni²⁺, Cd²⁺, Ag⁺, Ba²⁺, Mg²⁺, K⁺, Na⁺, and Li⁺; Supporting Information, Figures S17 and S18).

The solution of receptor 5/8 in THF/H₂O (9.5:0.5, v/v) is nonfluorescent when excited at 360 nm (Figure 2A/B). The quenched fluorescence emission is probably due to photo-induced electron transfer (PET) from the nitrogen atom of the spirolactam ring to the pentaquinone moiety. Interestingly, the

addition of incremental amounts of Hg²⁺ ions (0–200 equiv) to the solution of receptors 5 and 8 in THF/H₂O leads to the appearance of emission bands at 572 and 582 nm, respectively, due to the rhodamine (acceptor) moiety (Figure 2A/B). The emission intensity of receptor 5/8 increased linearly as a function of the Hg²⁺ ion concentration (inset, Figure 2A/B). We propose that emission enhancement at 572 and 582 nm is attributed to the opening of the spirolactam ring of rhodamine to the amide form, thus indicating the TBET process in receptors 5 and 8, i.e., via the conjugated linker from donor to acceptor (Scheme 2). The characteristic emission of the pentaquinone moiety at ~ 520 nm was not observed (Supporting Information, Figures S19 and S20), suggesting nearly 100% energy-transfer efficiency²⁶ within experimental error with large pseudo-Stokes shifts of up to 210 nm. We also carried out fluorescence titrations of compound 5/8 with Hg²⁺ ions at different pH values. It was observed that the compounds 5 and 8 operate well in the pH = 4.0–7.0 range (Supporting Information, Figures S21 and S22). Under sets of conditions similar to those for compounds 5 and 8, we also carried out fluorescence studies of an equimolar mixture of pentaquinone donor 6/9 and rhodamine acceptor 10 and found that no visible quenching of 6/9 and no enhancement in the fluorescence emission of the rhodamine acceptor was observed when the mixture was excited at the pentaquinone absorption band, i.e., at 360 nm, which clearly indicates that there is no

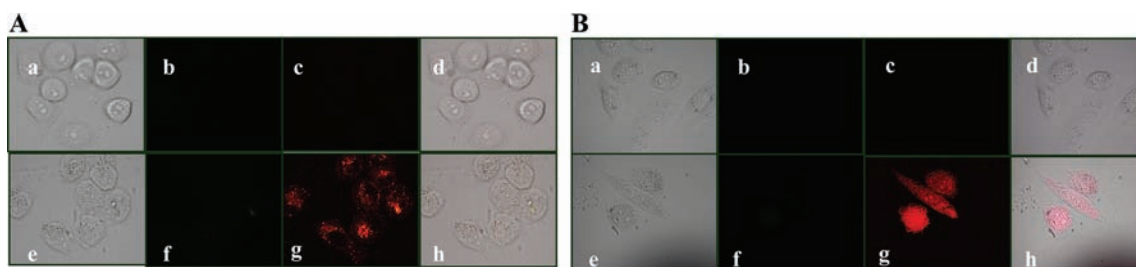


Figure 4. Fluorescence and bright-field images of PC3 cell lines: (a) bright-field image of cells treated with probe **8** ($1.0 \mu\text{M}$) only for 20 min at 37°C ; (b and c) fluorescence images of part a in green and red channels, respectively. (d) Overlay image of parts a–c; (e) bright-field image of cells upon treatment with probe **8** ($1.0 \mu\text{M}$) and then with $\text{Hg}(\text{ClO}_4)_2$ ($30.0 \mu\text{M}$) for 20 min; (f and g) fluorescence images of part e in green and red channels, respectively; (h) overlay image of parts e–g. (A) $\lambda_{\text{ex}} = 488 \text{ nm}$. (B) $\lambda_{\text{ex}} = 405 \text{ nm}$.

intermolecular energy transfer between the pentaquinone donor and rhodamine acceptor in the mixture (Supporting Information, Figures S23 and S24). Thus, the advantage of the TBET system for energy transfer is obvious. Further, for practical applications, it is very important that the fluorescence intensity of the acceptor in the cassette is greater than that of the acceptor without a donor when it is excited at the donor absorption wavelength. The fluorescence enhancement factors for receptors **5** and **8** are 56-fold and 160-fold, respectively, compared to **10** when excited at 360 nm (Supporting Information, Figures S25 and S26). Under the same conditions as those used above for Hg^{2+} , we also tested the fluorescence response of receptors **5** and **8** (Figure 3A/B) to other metal ions (Pb^{2+} , Cu^{2+} , Fe^{2+} , Fe^{3+} , Ni^{2+} , Zn^{2+} , Cd^{2+} , Co^{2+} , Mg^{2+} , Ba^{2+} , Ag^+ , K^+ , Na^+ , and Li^+), and a negligible change in fluorescence occurred in the presence of these metal ions (Supporting Information, Figures S27 and S28). The competitive experiments were conducted in the presence of 200 equiv of Hg^{2+} mixed with 200 equiv (Pb^{2+} , Cu^{2+} , Fe^{2+} , Fe^{3+} , Ni^{2+} , Zn^{2+} , Cd^{2+} , Co^{2+} , Mg^{2+} , Ba^{2+} , Ag^+ , K^+ , Na^+ , and Li^+) of various metal ions, respectively (Figure 3A/B), and no significant variation in the fluorescence intensity change was found by comparison with or without the other metal ions. Further, to study the influence of different counteranions such as Cl^- and NO_3^- , we examined the sensing behavior of receptor **5/8** with HgCl_2 and $\text{Hg}(\text{NO}_3)_2$. It was observed that there was no change in the sensing performance of the receptor **5/8** when these counteranions were used except in the case of receptor **8**, where there was a small decrease in the sensing performance when NO_3^- was used as the counterion (Supporting Information, Figures S29 and S30). The fluorescence quantum yields (Φ_{fs}) of compounds **5** and **8** in the free state were found to be 0.03 and 0.01, respectively, and the Hg^{2+} -bound states were found to be 0.15 and 0.21, respectively. Fitting the changes in the fluorescence spectra of compounds **5** and **8** with Hg^{2+} ions using the nonlinear regression analysis program *SPECFIT*²⁷ gave a good fit and demonstrated that 1:1 and 1:2 stoichiometry (host/guest) were the most stable species in the solution with the binding constant ($\log \beta$) = 5.00 and 7.92, respectively. The method of continuous variation (Job's plot; Supporting Information, Figures S31 and S32) was also used to prove the 1:1 and 1:2 stoichiometry, respectively.²⁸ The detection limits of compounds **5** and **8** as fluorescent sensors for analysis of the Hg^{2+} ions were found to be 5×10^{-6} and $7 \times 10^{-7} \text{ M}$, respectively, which were sufficiently low for detection of the submillimolar concentrations of Hg^{2+} ions, as found in many chemical systems. To test if the proposed complex could be reversed, we also carried out a reversibility experiment. The

addition of potassium iodide to the solutions of **5**– Hg^{2+} and **8**– Hg^{2+} complexes resulted in quenching of the fluorescence intensity. The quenching of fluorescence is due to the strong affinity of iodide ions for the Hg^{2+} ions, which resulted in decomplexation of the receptor– Hg^{2+} complex; i.e., Hg^{2+} ions were not available for binding with the receptor. Upon further addition of Hg^{2+} ions, the fluorescence was revived again along with the appearance of a pink color, which proved the reversible behavior of Hg^{2+} for receptors **5** and **8** (Supporting Information, Figures S33 and S34). To elucidate the binding mode of the receptor **5/8** with Hg^{2+} ions, the ^1H NMR spectrum of its complex with mercury perchlorate was also recorded. The protons corresponding to NCH_2CH_3 and NCH_2CH_3 undergo downshifts of 0.14/0.19 and 0.24/0.30 ppm, respectively, and the aromatic protons $\text{H}_{\text{c,d}}$, H_{e} , H_{f} and H_{g} corresponding to the rhodamine moiety of receptor **5/8** also undergo downfield shifts of 0.34/0.44, 0.22/0.31, 0.07/0.26, and 0.03/0.24 ppm, respectively, in the presence of 1.0/2.0 equiv of Hg^{2+} ions. (Supporting Information, Figures S35 and S36), which indicates transformation of the nonfluorescent spirocyclic form of the rhodamine moiety in receptor **5/8** to the fluorescent ring-opened amide form (Scheme 2).

The potential biological application of receptor **8** was evaluated for the in vitro detection of Hg^{2+} ions in prostate cancer (PC3) cell lines (Figure 4A,B). The prostate cancer (PC3) cell lines were incubated with receptor **8** [$1.0 \mu\text{M}$ in $\text{THF}/\text{H}_2\text{O}$ (9.5:0.5, v/v) buffered with HEPES, $\text{pH} = 7.0$] in a RPMI-1640 medium for 20 min at 37°C and washed with a phosphate-buffered saline (PBS) buffer ($\text{pH} = 7.4$) to remove excess receptor **8**. Microscopic images showed no fluorescence in both the green and red channels respectively as shown in Figure 4A,B (b–c). The cells were then treated with mercury perchlorate ($30.0 \mu\text{M}$) in the RPMI-1640 medium, incubated again for 20 min at 37°C , and washed with a PBS buffer. After treatment with Hg^{2+} ions, the cells showed significant red fluorescence emission [Figure 4A,B (g)]. These results suggest that **8** is an effective intracellular Hg^{2+} imaging agent with the appearance of red emission attributed to the working of the TBET phenomenon within the cells.

CONCLUSION

In conclusion, new rhodamine–pentaquinone dyad **5** and rhodamine–pentaquinone–rhodamine triad **8** have been synthesized that show TBET in the presence of Hg^{2+} ions in mixed aqueous solution. Complexation of the Hg^{2+} ion opens the spirocyclic ring of rhodamine moieties to give specific color change as well as fluorescence enhancement at 572 and 582 nm, respectively. In addition, in vitro properties of

compound **8** showed good selectivity toward Hg^{2+} ions with “on” fluorescence response.

EXPERIMENTAL SECTION

General Information. All reagents were purchased from Aldrich and were used without further purification. THF (AR grade) was used to perform analytical studies. UV–vis spectra were recorded on a Shimadzu UV-2450 spectrophotometer with a quartz cuvette (path length, 1 cm). The fluorescence spectra were recorded with a Varian Cary Eclipse spectrofluorimeter. ^1H and ^{13}C NMR spectra were recorded on a JEOL-FT NMR-AL 300 MHz using CDCl_3 as the solvent and tetramethylsilane (SiMe_4) as internal standards. Data are reported as follows: chemical shifts in ppm (δ), multiplicity (s = singlet, d = doublet, q = quartet, br = broad singlet, m = multiplet, dd = doublet of doublet), coupling constants (Hz), integration, and interpretation. Silica gel 60 (60–120 mesh) was used for column chromatography. The fluorescence quantum yield²⁹ was determined using optically matching solutions of rhodamine B ($\Phi_{fr} = 0.65$ in ethanol) as standards at an excitation wavelength of 540 nm, and the quantum yield is calculated using the equation

$$\Phi_{fs} = \Phi_{fr} \times \frac{1 - 10^{-A_s L_s}}{1 - 10^{-A_r L_r}} \times \frac{N_s^2 / N_r^2}{D_s / D_r}$$

Φ_{fs} and Φ_{fr} are the radiative quantum yields of the sample and reference, respectively, A_s and A_r are the absorbances of the sample and reference, respectively, D_s and D_r are the respective areas of emission for the sample and reference, respectively, L_s and L_r are the lengths of the absorption cells of the sample and reference, respectively, and N_s and N_r are the refractive indices of the sample and reference solutions (pure solvents were assumed), respectively.

Procedure for Metal-Ion Sensing. Solutions of compounds **5**, **6**, **8**, **9**, and **11** and metal perchlorates were prepared in THF/ H_2O (9.5:0.5, v/v) buffered with HEPES, pH = 7.0. In titration experiments, each time a 3 mL solution of **5/8** (10 μM) was filled in a quartz cuvette (path length, 1 cm) and metal ions were added into the quartz cuvette by using a micropipet. For fluorescence measurements, excitation was provided at 360 nm, and emission was collected from 350 to 650 nm.

Procedure for Fluorescence Imaging. The prostate cancer (PC3) cell lines were incubated with receptor **8** [1.0 μM in THF/ H_2O (9.5:0.5, v/v) buffered with HEPES, pH = 7.0] in a RPMI-1640 medium for 20 min at 37 °C and washed with a PBS buffer (pH = 7.4) to remove excess receptor **8**. The cells were then treated with mercury perchlorate (30.0 μM) in the RPMI-1640 medium, incubated again for 20 min at 37 °C, and washed with a PBS buffer. The cells were imaged by a confocal fluorescence microscope with excitation wavelengths of 488 and 405 nm.

Compounds **2**,²² **7**,²¹ and **11**²⁵ were synthesized according to the literature procedure.

2-(4-Aminophenyl)-6,13-pentacenequinone (3). To a solution of **1** (0.6 g, 1.55 mmol) and **2** (0.41 g, 1.87 mmol) in dry dioxane were added K_2CO_3 (0.42 g, 3.1 mmol), H_2O (10 mL), and $[\text{Pd}(\text{Cl})_2(\text{PPh}_3)_2]$ (0.271 g, 0.25 mmol) under N_2 . The mixture was degassed and purged with N_2 for 15 min. The mixture was refluxed overnight. The dioxane was then removed under vacuum, and the residue so obtained was treated with water, extracted with dichloromethane, and dried over anhydrous Na_2SO_4 . The organic layer was evaporated, and the compound was purified by column chromatography using $\text{CHCl}_3/\text{MeOH}$ (9.5:0.5, v/v) as an eluent to give 0.20 g (32%) of compound **3** as a red solid. Mp: >260 °C. ^1H NMR (300 MHz, CDCl_3 , ppm): δ 3.89 (br, 2H, NH_2), 6.84 (d, 2H, $J = 8.4$, ArH), 7.59–7.73 (m, 4H, ArH), 7.94 (d, 1H, $J = 7.8$, ArH), 8.12–8.16 (m, 3H, ArH), 8.24 (s, 1H, ArH), 8.93–8.98 (m, 4H, ArH). TOF-ES⁺-MS: m/z 400.12 [($M + 1$)⁺]. Anal. Calcd for $\text{C}_{28}\text{H}_{17}\text{NO}_2$: C, 84.19; H, 4.29; N, 3.51. Found: C, 83.95; H, 4.32; N, 3.33.

2-(*N*-Phenylrhodamine B)-6,13-pentacenequinone (5). The acid chloride **4**²⁴ (0.15 g, 0.3 mmol) was added to the stirred solution of **3** (0.1 g, 0.25 mmol) in dry THF and triethylamine. The reaction mixture was stirred overnight at room temperature. The reaction mixture was treated with water, extracted with dichloromethane, and

dried over anhydrous Na_2SO_4 . The organic layer was evaporated under reduced pressure, and the crude product was purified by column chromatography (EtOAc/hexane, 1:4, v/v) to give 70 mg (34%) of compound **5** as a yellow solid. Mp: >250 °C. ^1H NMR (300 MHz, CDCl_3 , ppm): δ 1.16 (t, 12H, $J = 7.05$, CH_3), 3.29–3.37 (q, 8H, NCH_2), 6.28–6.36 (m, 4H, ArH), 6.69 (d, 2H, $J = 9.3$, ArH), 7.08 (d, 2H, $J = 7.5$, ArH), 7.17 (d, 1H, $J = 6.6$, ArH), 7.50–7.53 (m, 4H, ArH), 7.68–7.70 (m, 2H, ArH), 7.71–7.82 (m, 1H, ArH), 8.02–8.16 (m, 5H, ArH), 8.88–8.92 (m, 4H, ArH). ^{13}C NMR (75.45 MHz, CDCl_3 , cm^{-1}): δ 12.56, 44.29, 67.50, 97.88, 108.25, 123.40, 123.99, 127.06, 127.47, 128.18, 128.74, 128.82, 129.32, 129.55, 129.73, 129.99, 130.28, 130.48, 130.57, 130.72, 133.01, 134.02, 135.08, 135.13, 135.35, 148.87, 153.07, 167.93, 182.67. TOF-ES⁺-MS: m/z 824.3 [($M + 1$)⁺]. Anal. Calcd for $\text{C}_{56}\text{H}_{45}\text{N}_3\text{O}_4$: C, 81.63; H, 5.50; N, 5.10. Found: C, 81.78; H, 5.35; N, 5.25.

2-(*N*-Phenylacetamide)-6,13-pentacenequinone (6). To a solution of **3** (0.03 g, 0.075 mmol) in acetic acid (5.0 mL) was added an excess of acetic anhydride in ice-cold conditions, and the resulting reaction mixture was stirred at room temperature for 2 h. The reaction mixture was then poured into ice-cold water for precipitation. The precipitate thus formed was filtered, washed with water, and dried to give 32 mg (91%) of compound **6** as a yellow solid. Mp: >250 °C. ^1H NMR (300 MHz, CDCl_3 , ppm): δ 2.10 (s, 3H, CH_3), 7.73–7.87 (m, 6H, ArH), 8.08–8.11 (m, 1H, ArH), 8.31–8.35 (m, 2H, ArH), 8.39 (s, 1H, ArH), 8.59 (s, 1H, ArH), 8.90–8.95 (m, 4H, ArH); Anal. Calcd for $\text{C}_{30}\text{H}_{19}\text{NO}_3$: C, 81.62; H, 4.34; N, 3.17. Found C, 81.49; H, 4.45; N, 3.39. IR (KBr, cm^{-1}): ν_{max} 1674 (C=O).

2,3-Bis(di-*N*-phenylrhodamine B)-6,13-pentacenequinone (8). The acid chloride **4**²⁴ (0.11 g, 0.22 mmol) was added to the stirred solution of diamine **7** (0.05 g, 0.10 mmol) in dry THF and triethylamine. The reaction mixture was stirred overnight at room temperature. The reaction mixture was treated with water, extracted with dichloromethane, and dried over anhydrous Na_2SO_4 . The organic layer was evaporated under reduced pressure, and the crude product was purified by column chromatography (EtOAc/hexane, 1:1, v/v) to give 138 mg (50%) of compound **8** as a yellow solid. Mp: >250 °C. ^1H NMR (300 MHz, CDCl_3 , ppm): δ 1.11 (t, 24H, $J = 6.9$, CH_3), 3.26–3.33 (q, 16H, NCH_2), 6.28–6.31 (m, 8H, ArH), 6.61 (d, 4H, $J = 9.3$, ArH), 6.83 (d, 4H, $J = 8.4$, ArH), 6.94 (d, 4H, $J = 8.4$, ArH), 7.15–7.17 (m, 2H, ArH), 7.49–7.51 (m, 4H, ArH), 7.68–7.71 (m, 2H, ArH), 7.96 (s, 2H, ArH), 8.0–8.02 (m, 2H, ArH), 8.10–8.13 (m, 2H, ArH), 8.86 (s, 2H, ArH), 8.93 (s, 2H, ArH). ^{13}C NMR (75.45 MHz, CDCl_3 , cm^{-1}): δ 13.01, 44.72, 68.07, 98.38, 107.09, 108.62, 123.74, 124.37, 126.45, 128.49, 128.97, 129.81, 130.01, 130.32, 130.43, 130.98, 131.06, 131.23, 132.04, 133.25, 134.69, 135.58, 136.99, 137.82, 142.37, 149.18, 153.55, 153.80, 167.97, 183.16. MALDI-TOF: m/z 1338.36 [(M)⁺]. Anal. Calcd for $\text{C}_{90}\text{H}_{78}\text{N}_6\text{O}_6$: C, 80.69; H, 5.87; N, 6.27. Found: C, 80.43; H, 5.65; N, 6.56.

2,3-Bis(di-*N*-phenylacetamide)-6,13-pentacenequinone (9). To a solution of **7** (0.03 g, 0.06 mmol) in acetic acid (5.0 mL) was added an excess of acetic anhydride in ice-cold conditions, and the resulting reaction mixture was stirred at room temperature for 2 h. The reaction mixture was then poured into ice-cold water for precipitation. The precipitate thus formed was filtered, washed with water, and dried to give 0.02 g (57%) of compound **9** as a yellow solid. Mp: >250 °C; ^1H NMR (300 MHz, CDCl_3 , ppm): δ 2.20 (s, 6H, CH_3), 7.20 (d, 4H, $J = 6.03$, ArH), 7.44 (d, 4H, $J = 6.27$, ArH), 7.73 (br, 2H, ArH), 8.13 (br, 4H, ArH), 8.97 (s, 4H, ArH); TOF-ES⁺-MS: 575.3 [($M + 1$)⁺]. Anal. Calcd for $\text{C}_{38}\text{H}_{26}\text{N}_2\text{O}_4$: C, 79.43; H, 4.56; N, 4.88. Found: C, 79.1; H, 4.24; N, 4.95. IR (KBr, cm^{-1}): ν_{max} 1666 (C=O).

ASSOCIATED CONTENT

Supporting Information

Characterization data including ^1H and ^{13}C NMR, IR, MS, UV–vis, fluorescence spectra and energy transfer efficiency calculation. This material is available free of charge via the Internet at <http://pubs.acs.org>.

■ AUTHOR INFORMATION

Corresponding Author

*E-mail: vanmanan@yahoo.co.in (V.B.), mksharmaa@yahoo.co.in (M.K.). Tel.: 91182258802 ext. 3302.

■ ACKNOWLEDGMENTS

We are thankful to CSIR (New Delhi, India) for financial support [Reference No. CSIR Scheme 01 (2167)07/EMR-II]. We are also thankful to Central Drug Research Institute (CDRI), Lucknow, India, for ES⁺-MS spectra and to Guru Nanak Dev University for providing research facilities. Roopa is thankful to CSIR (New Delhi, India) for a senior research fellowship.

■ REFERENCES

- (1) (a) Martinez-Manez, R.; Sancenon, F. *Chem. Rev.* **2003**, *103*, 4449. (b) Czarnik, A. W. *Acc. Chem. Res.* **1994**, *27*, 302. (c) Kim, J. S.; Quang, D. T. *Chem. Rev.* **2007**, *107*, 3780. (d) Sinkeldam, R. W.; Greco, N. J.; Tor, Y. *Chem. Rev.* **2010**, *110*, 2579. (e) *Fluorescent Chemosensors for Ion and Molecule Recognition*; Czarnik, A. W., Ed.; American Chemical Society: Washington, DC, 1992.
- (2) de Silva, A. P.; Gunaratne, H. Q. N.; Gunnlaugsson, T.; Huxley, A. J. M.; McCoy, C. P.; Rademacher, J. T.; Rice, T. E. *Chem. Rev.* **1997**, *97*, 1515.
- (3) Benoit, J. M.; Fitzgerald, W. F.; Damman, A. W. *Environ. Res.* **1998**, *78*, 118.
- (4) Benzoni, A.; Zino, F.; Franchi, E. *Environ. Res.* **1998**, *77*, 68.
- (5) *Mercury Update: Impact on Fish Advisories*; EPA Fact Sheet EPA-823-F-01-001; Environmental Protection Agency, Office of Water: Washington, DC, 2001.
- (6) Malm, O. *Environ. Res.* **1998**, *77*, 73.
- (7) (a) Grandjean, P.; Weihe, P.; White, R. F.; Debes, F. *Environ. Res.* **1998**, *77*, 165. (b) Takeuchi, T.; Morikawa, N.; Matsumoto, H.; Shiraishe, Y. *Acta Neuropathol.* **1962**, *2*, 40. (c) Harada, M. *Crit. Rev. Toxicol.* **1995**, *25*, 1.
- (8) Harris, H. H.; Pickering, I. J. P.; George, G. N. *Science* **2003**, *301*, 1203.
- (9) Gutknecht, J. J. *Membr. Biol.* **1981**, *61*, 61.
- (10) McClure, D. S. *J. Chem. Phys.* **1952**, *20*, 682.
- (11) Rurack, K.; Resch-Genger, U.; Rettig, W. *J. Photochem. Photobiol., A* **1998**, *118*, 143.
- (12) (a) Yoon, S.; Albers, A. E.; Wong, A. P.; Chang, C. J. *J. Am. Chem. Soc.* **2005**, *127*, 16030. (b) Yoon, S.; Miller, E. W.; He, Q.; Do, P. K.; Chang, C. J. *Angew. Chem., Int. Ed.* **2007**, *46*, 6658.
- (13) (a) Zhang, M.; Yu, M. X.; Li, F. Y.; Zhu, M. W.; Li, M. Y.; Gao, Y. H.; Li, L.; Liu, Z. Q.; Zhang, J. P.; Zhang, D. Q.; Yi, T.; Huang, C. H. *J. Am. Chem. Soc.* **2007**, *129*, 10322. (b) Sasaki, E.; Kojima, H.; Nishimatsu, H.; Urano, Y.; Kikuchi, K.; Hirata, Y.; Nagano, T. *J. Am. Chem. Soc.* **2005**, *127*, 3684. (c) Yang, D.; Wang, H. L.; Sun, Z. N.; Chung, N. W.; Shen, J. G. *J. Am. Chem. Soc.* **2006**, *128*, 6004. (d) Lim, N. C.; Freake, H. C.; Bruckner, C. *Chem.—Eur. J.* **2005**, *11*, 38. (e) Zhang, G.; Zhang, D.; Yin, S.; Yang, X.; Shuai, Z.; Zhu, D. *Chem. Commun.* **2005**, 2161. (f) Liu, L.; Zhang, G.; Xiang, J.; Zhang, D.; Zhu, D. *Org. Lett.* **2008**, *10*, 4581. (g) Wang, C.; Zhang, D.; Zhang, G.; Xiang, J.; Zhu, D. *Chem.—Eur. J.* **2008**, *14*, 5680.
- (14) (a) Xiang, Y.; Tong, A.; Jin, P.; Ju, Y. *Org. Lett.* **2006**, *8*, 2863. (b) Zhang, X.; Shiraishe, Y.; Hirai, T. *Org. Lett.* **2007**, *9*, 5039. (c) Yang, Y. K.; Yook, K. J.; Tae, J. *J. Am. Chem. Soc.* **2005**, *127*, 16760. (d) Shi, W.; Ma, H. *Chem. Commun.* **2008**, *16*, 1856. (e) Kim, H. A.; Lee, M. H.; Kim, H. J.; Kim, J. S. *Chem. Soc. Rev.* **2008**, *37*, 1465. (f) Beija, M.; Afonso, C. A. M.; Martinho, J. M. G. *Chem. Soc. Rev.* **2009**, *38*, 2410. (g) Lou, X.; Zhang, Y.; Li, Q.; Qin, J.; Li, Z. *Chem. Commun.* **2011**, *47*, 3189.
- (15) (a) Tolosa, L.; Nowaczyk, K.; Lakowicz, J. *An Introduction to Laser Spectroscopy*, 2nd ed.; Kluwer: New York, 2002. (b) Zhang, X.; Xiao, Y.; Qian, X. *Angew. Chem.* **2008**, *120*, 8145; *Angew. Chem., Int. Ed.* **2008**, *47*, 8025.
- (16) (a) Othman, A. B.; Lee, J. W.; Wu, J.-S.; Kim, J. S.; Abidi, R.; Thurey, P.; Strub, J. M.; Drosselaer, A. V.; Vicens, J. *J. Org. Chem.* **2007**, *72*, 7634. (b) Zhou, Z.; Yu, M.; Yang, H.; Huang, K.; Li, F.; Yi, T.; Huang, C. *Chem. Commun.* **2008**, 3387. (c) Lee, M. H.; Kim, H. J.; Yoon, S.; Park, N.; Kim, J. S. *Org. Lett.* **2008**, *10*, 213. (d) Jisha, V. S.; Thomas, A. J.; Ramaiah, D. *J. Org. Chem.* **2009**, *74*, 6667. (e) Xu, M.; Wu, S.; Zeng, F.; Yu, C. *Langmuir* **2010**, *26*, 4529. (f) Kaewtong, C.; Noisepphum, J.; Upaa, Y.; Morakot, N.; Wannoo, B.; Tuntulani, T.; Pulpoka, B. *New J. Chem.* **2010**, *34*, 1104. (g) Yu, H.; Fu, M.; Xiao, Y. *Phys. Chem. Chem. Phys.* **2010**, *12*, 7386. (h) Kumar, M.; Kumar, N.; Bhalla, V. *Tetrahedron Lett.* **2011**, *52*, 4333.
- (17) (a) Jiao, G.-S.; Thorensen, L. H.; Burgess, K. *J. Am. Chem. Soc.* **2003**, *125*, 14668. (b) Bandichhor, R.; Petrescu, A. D.; Vespa, A.; Kier, A. B.; Schroeder, F.; Burgess, K. *J. Am. Chem. Soc.* **2006**, *128*, 10688. (c) Han, J.; Josh, J.; Mei, E.; Burgess, K. *Angew. Chem., Int. Ed.* **2007**, *46*, 1684. (d) Lin, W.; Yuan, L.; Cao, Z.; Feng, Y.; Song, J. *Angew. Chem., Int. Ed.* **2010**, *49*, 375.
- (18) Kumar, M.; Kumar, N.; Bhalla, V.; Singh, H.; Sharma, P. R.; Kaur, T. *Org. Lett.* **2011**, *13*, 1422.
- (19) (a) Kumar, M.; Dhir, A.; Bhalla, V.; Sharma, R.; Puri, R. K.; Mahajan, R. K. *Analyst* **2010**, *135*, 1600. (b) Kumar, R.; Bhalla, V.; Kumar, M. *Tetrahedron* **2008**, *64*, 8095. (c) Bhalla, V.; Tejpal, R.; Kumar, M.; Sethi, A. *Inorg. Chem.* **2009**, *48*, 11677. (d) Bhalla, V.; Singh, H.; Kumar, M. *Org. Lett.* **2010**, *12*, 628. (e) Kumar, M.; Dhir, A.; Bhalla, V. *Eur. J. Org. Chem.* **2009**, 4534. (f) Kumar, M.; Dhir, A.; Bhalla, V. *Tetrahedron* **2009**, *65*, 7510. (g) Dhir, A.; Bhalla, V.; Kumar, M. *Tetrahedron Lett.* **2008**, *49*, 4227. (h) Dhir, A.; Bhalla, V.; Kumar, M. *Org. Lett.* **2008**, *10*, 4891. (i) Kumar, M.; Dhir, A.; Bhalla, V. *Org. Lett.* **2009**, *11*, 2567. (j) Kumar, M.; Kumar, R.; Bhalla, V. *Chem. Commun.* **2009**, 7384. (k) Kumar, M.; Kumar, R.; Bhalla, V. *Tetrahedron Lett.* **2010**, *51*, 5559. (l) Bhalla, V.; Gupta, A.; Roopa; Singh, H.; Kumar, M. *J. Org. Chem.* **2011**, *76*, 1578.
- (20) Lehnerr, D.; Gao, J.; Hegmann, F. A.; Tykwinski, R. R. *Org. Lett.* **2008**, *10*, 4779.
- (21) Bhalla, V.; Roopa; Gupta, A.; Dhir, A.; Kumar, M. *Dalton Trans.* **2011**, *40*, 5176.
- (22) Bhalla, V.; Tejpal, R.; Kumar, M.; Puri, R. K.; Mahajan, R. K. *Tetrahedron Lett.* **2009**, *50*, 2649.
- (23) Swartz, C. R.; Parkin, S. R. J.; Bullock, E.; Anthony, J. E. *Org. Lett.* **2005**, *7*, 3163.
- (24) Huang, J.; Xu, Y.; Qian, X. *J. Org. Chem.* **2009**, *74*, 2167.
- (25) Dujols, V.; Ford, F.; Cazarnik, A. W. *J. Am. Chem. Soc.* **1997**, *119*, 7386.
- (26) Actual energy-transfer efficiencies in compounds **5** and **8** are 98.28% and 99.49%, respectively.
- (27) Gampp, H.; Maeder, M.; Meyer, C. J.; Zuberbulher, A. D. *Talanta* **1985**, *32*, 95.
- (28) Job, P. *Ann. Chim.* **1928**, *9*, 113.
- (29) Deams, J. N.; Grosby, G. A. *J. Phys. Chem.* **1971**, *75*, 991.